NASA/TM—1999-208899

Thermal-Mechanical Stability of Single Crystal Oxide Refractive Concentrators for High-Temperature Solar Thermal Propulsion

Dongming Zhu, Nathan S. Jacobson, and Robert A. Miller
Lewis Research Center, Cleveland, Ohio

Prepared for the
1999 International Solar Energy Conference, Renewable and Advanced Energy Systems for the 21st Century
sponsored by the American Society of Mechanical Engineers
Lahaina, Maui, Hawaii, April 11–15, 1999

National Aeronautics and
Space Administration

Lewis Research Center

February 1999

Acknowledgments

Concentrator development project,
hors are grateful to

This work was supported by NASA Lewis Research Center Refractive Secondary Solar
and NASA Marshall Space Flight Center shooting Star Program. The au
Robert P. Macosko for valuable discussions.

Available from

nal Technical Information Service
5285 Port Royal Road
Springfield, VA 22100
Price Code: A03

NASA Center for Aerospace Information
7121 Standard Drive
Hanover, MD 21076
Price Code: A03

Natio

Thermal-Mechanical Stability of Single Crystal Oxide Refractive Concentrators for High-Temperature Solar Thermal Propulsion

Dongming Zhu
Ohio Aerospace Institute
Brook Park, OH 44142
E-mail:Dongming.Zhu@lerc.nasa.gov

Nathan S. Jacobson and Robert A. Miller
NASA Lewis Research Center
21000 Brookpark Road
Cleveland, OH 44135

ABSTRACT

Single crystal oxides such as yttria-stabilized zirconia (Y_2O_3-ZrO_2), yttrium aluminum garnet ($Y_3Al_5O_{12}$, or YAG), magnesium oxide (MgO) and sapphire (Al_2O_3) are candidate refractive secondary concentrator materials for high temperature solar propulsion applications. However, thermo-mechanical reliability of these components in severe thermal environments during the space mission sun/shade transition is of great concern. Simulated mission tests are important for evaluating these candidate oxide materials under a variety of transient and steady-state heat flux conditions, and thus provide vital information for the component design. In this paper, a controlled heat flux thermal shock test approach is established for the single crystal oxide materials using a 3.0 kW continuous wave CO_2 laser, with a wavelength 10.6 micron. Thermal fracture behavior and failure mechanisms of these oxide materials are investigated and critical temperature gradients are determined under various temperature and heating conditions. The test results show that single crystal sapphire is able to sustain the highest temperature gradient and heating-cooling rate, and thus exhibit the best thermal shock resistance, as compared to the yttria-stabilized zirconia, yttrium aluminum garnet and magnesium oxide.

INTRODUCTION

Recently refractive secondary solar concentrator systems have been developed for solar thermal power and propulsion applications [1]. A well-designed refractive

secondary concentrator system possesses higher solar concentration ratio and efficiency, and better flux tailoring within the heat receiver cavity, as compared to the conventional hollow reflective parabolic concentrator systems [1, 2]. Single crystal oxides such as yttria-stabilized zirconia (Y_2O_3-ZrO_2), yttrium aluminum garnet ($Y_3Al_5O_{12}$, or YAG), magnesium oxide (MgO) and sapphire (Al_2O_3) are candidate refractive secondary concentrator materials. However, the refractive concentrator system will experience high temperature and thermal cycling in the solar thermal engine during the space mission sun/shade transition and therefore thermal mechanical reliability of the oxide components in the severe thermal environments is of great concern. Finite element analysis shows that for a cubic ZrO_2-Y_2O_3 single crystal concentrator system, a peak temperature of 1800°C at the tip of the concentrator flux extractor and a temperature difference up to 1500°C across the 25.4 mm region of the concentrator-extractor interface may be established during the heat-up cycles [3].

The purpose of this paper is to establish appropriate test techniques to evaluate the thermo-mechanical stability of four different candidate single crystal oxide materials, under space mission thermal gradient and heat flux conditions. Thermal stress resistance, thermal fracture behavior and failure mechanisms of these single crystal are investigated under steady-state and transient heat flux conditions. Critical temperature gradients and corresponding absorbed power densities imposed on the crystals to cause failure, are determined for various temperature and heating conditions that these materials are expected to experience in refractive concentrator applications.

EXPERIMENTAL MATERIALS AND METHODS

Materials

Single crystal oxides including 20%Y_2O_3-doped cubic zirconia (Y_2O_3-ZrO_2), yttrium aluminum garnet ($Y_3Al_5O_{12}$ or YAG), magnesium oxide (MgO) and sapphire (Al_2O_3) were obtained from a commercial source (ONYX Optics, Inc., 6551 Sierra lane, Dublin, California). The materials were machined into 25.4 mm diameter circular disk specimens (thickness 1 mm), and 12.7 mm diameter cylindrical specimens (length 12.7

mm or 25.4 mm). The surfaces of the disk and cylinder specimens were parallel to the major crystallographic planes of these crystals, namely, (100) plane for ZrO_2-Y_2O_3 and MgO, (111) plane for YAG, and (0001) plane for Al_2O_3 (sapphire). These surface plane directions of the specimens were thus consistent with the optical axes of the actual components. For the ZrO_2-Y_2O_3 and MgO materials, $12.7 \times 12.7 \times 12.7$ mm cube specimens with the (100) orientation surfaces were also used. The crystallographic orientations of the specimen surfaces were confirmed using X-ray Laue diffraction. Specimen surfaces were polished to a mirror finish on all sides before each test.

Thermal Expansion and Room Temperature Hardness Tests

Thermal expansion experiments were carried out on all the single crystals, in air, using a high temperature dilatometer system. The 25.4 mm-long cylindrical specimens were used for the thermal expansion measurements, and a platinum standard specimen was used as reference. Since yttria-doped ZrO_2, MgO and YAG have cubic structures, and it is normally assumed that these materials are isotropic, the material thermal expansions were measured only in their component optical axis directions ([100] direction for ZrO_2 and MgO, and [111] direction for YAG). For anisotropic sapphire, however, thermal expansions were measured not only in the optical axis direction [0001] using the 25.4 mm-long cylindrical specimen, but also in the directions perpendicular to its [0001] axis using the 25.4 mm diameter thin disk specimens.

Room-temperature Knoop hardness tests were conducted using a Knoop indenter on yttra-doped ZrO_2 (100), MgO (100), YAG (111) and Al_2O_3 (0001) surfaces, in accordance with ASTM C1326. The load used was 500 g and dwell time was 15 seconds. For each specimen, a total of twenty measurements were made, and average hardness values were obtained for the materials.

The Steady-State Thermal Gradient Test and Transient Thermal Shock Test

A 3.0 kW CO_2 continuous wave (wavelength 10.6 μm) laser was used to provide controlled surface heating for the oxide specimens. A schematic diagram of the laser test rig used for this high-temperature thermal gradient testing is illustrated in Figure 1. The

CO_2 laser is especially well-suited for the single crystal thermal shock tests because it can directly deliver well-characterized heat energy to the oxide surfaces. Since the oxides are opaque at the 10.6 μm wavelength of laser beam, the light energy is absorbed at the surfaces rather than transmitting into the crystals, and thus generating the required temperature gradients within the specimens. In order to provide more uniform heating over the entire specimen surface, the relatively sharp raw beam with a diameter of 13 mm was expanded to a broader beam size with a diameter of 40 mm, using a ZnSe (focal length 63.5 mm) positive meniscus lens. The resulting laser beam profile was measured on a PC laser beam analyzer by capturing a thermal image of a 0.5-second laser pulse. The measured power density distribution of the expanded laser beam is shown in Figure 2. Despite of a 15% difference in the laser beam energy distribution between the peak and valley, a fairly uniform surface heating was observed by thermography even for the 25.4 mm diameter disk specimens.

Steady-state thermal gradient tests were conducted on the thin disk specimens to determine the critical temperature differences across the specimen thickness to initiate cracking. A temperature gradient was established through the specimen thickness by laser direct surface heating and backside air cooling. The laser power (thus the heat flux) was continuously increased at a slow rate, so a pseudo-steady-state heating of the specimen was always achieved and the temperature gradient across the specimen thickness increased with the heating time. Since the disk specimen immediately broke off once the crack was initiated, the onset of the cracking and fracture of the specimen was recorded as a sudden temperature drop in the pyrometer temperature reading. The specimen failure temperatures can be roughly controlled by adjusting the cooling. The critical temperature difference was thus determined for each specimen at various specimen back temperatures.

The thermal gradient testing of the single crystal cylindrical specimens was also carried out to simulate the heating/cooling cycles during the space mission. In this experiment, indirect laser heating (by laser-heated superalloy plate thermal conduction) was used to ensure extremely slow surface heating (Figure 1 (b)). Surface temperature

was measured by a type-R thermocouple at the back side of the laser heated superalloy heating plate near the specimen. Specimen cracking was monitored from a video camera and real-time thermography images. The specimens were inspected after each cycle.

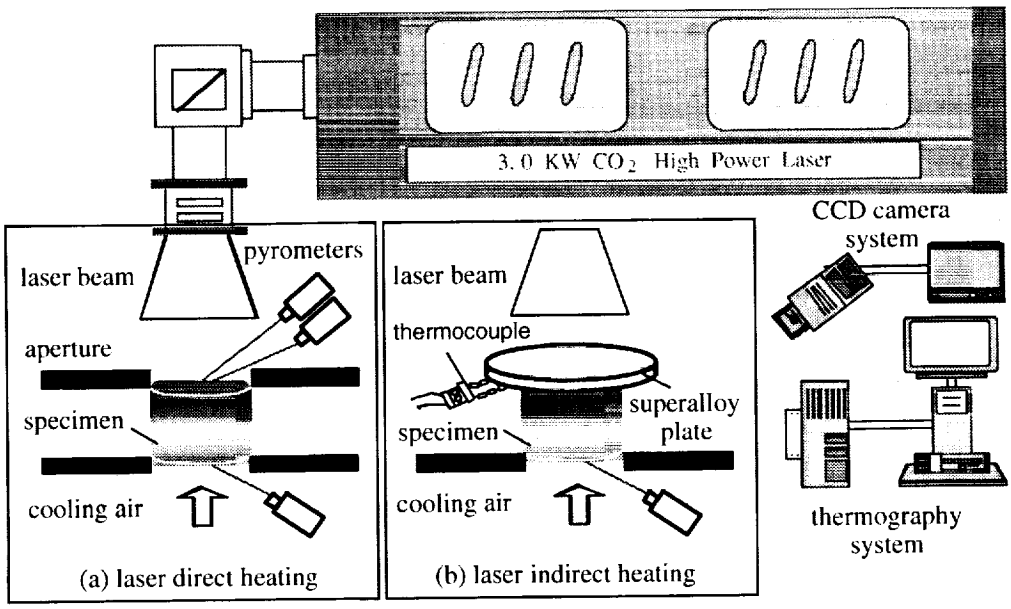

Fig.1 Schematic diagram showing high temperature thermal gradient testing of candidate refractive solar concentrator oxide materials using a high power laser. The laser power is measured using an internal power meter. The surface and back temperatures, and temperature distributions of the specimen are monitored by 8-μm pyrometers, and a 3 μm thermography unit. Thermocouples are also used in temperature measurements of laser indirect heating. All data are recorded in a computer system.

Laser transient thermal shock tests were conducted on the cylindrical single crystal specimens using a direct laser beam heating approach. Laser power was increased in approximately 30 W increments and the specimen was heated for a total time of 60 seconds. Specimen cracking was also monitored using a video camera and real-time thermography. The critical laser power density resulting in specimen fracture was thus determined for each specimen. For each material, two specimens were tested and an average critical power value was chosen. During the test, heating/cooling profiles and

temperature distributions were experimentally measured with thermography and pyrometry, and were also compared with the analytical solutions [4] and one-dimensional (one–D) finite difference models described previously [5, 6].

Microstructural evidence to help explain thermal fracture behavior and failure mechanisms of these oxide materials was examined after each test using optical and scanning electron microscopy.

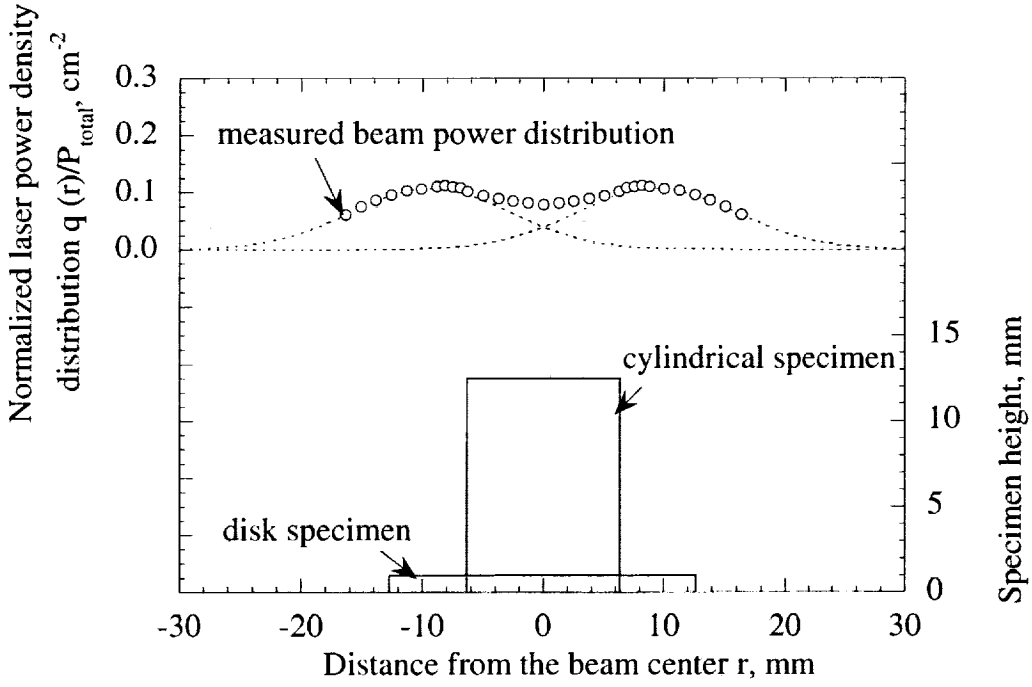

Fig. 2 The measured power density distribution $q(r)$ of the expended laser beam. Note that the power density distribution shown is normalized with respected to the total laser power P.

EXPERIMENTAL RESULTS AND DISCUSSION

Figure 3 shows the thermal expansion behavior of the single crystal materials up to a temperature of 1400°C. It can be seen that MgO has the highest coefficient of thermal expansion (CTE), while sapphire has the lowest coefficient of thermal expansion (CTE).

The average CTE values for these materials are: 10.6×10^{-6} m/m - °C for yttria-doped ZrO_2, 9.2×10^{-6} m/m - °C for YAG, 13.8×10^{-6} m/m - °C for MgO, 8.9×10^{-6} m/m - °C for Al_2O_3 parallel to [0001] direction and 8.6×10^{-6} m/m - °C for Al_2O_3 perpendicular to [0001], respectively.

Figure 4 shows the room-temperature hardness measurement results. Among these oxides, Al_2O_3 has the highest hardness, whereas MgO has the lowest hardness. Yttria-doped ZrO_2 and YAG have almost equivalent hardness values. The average Knoop hardness values are 11.25 ± 0.39GPa for Y_2O_3-doped ZrO_2, 11.13 ± 0.37GPa for YAG, 3.73 ± 0.24GPa for MgO, 15.01 ± 0.53GPa for Al_2O_3.

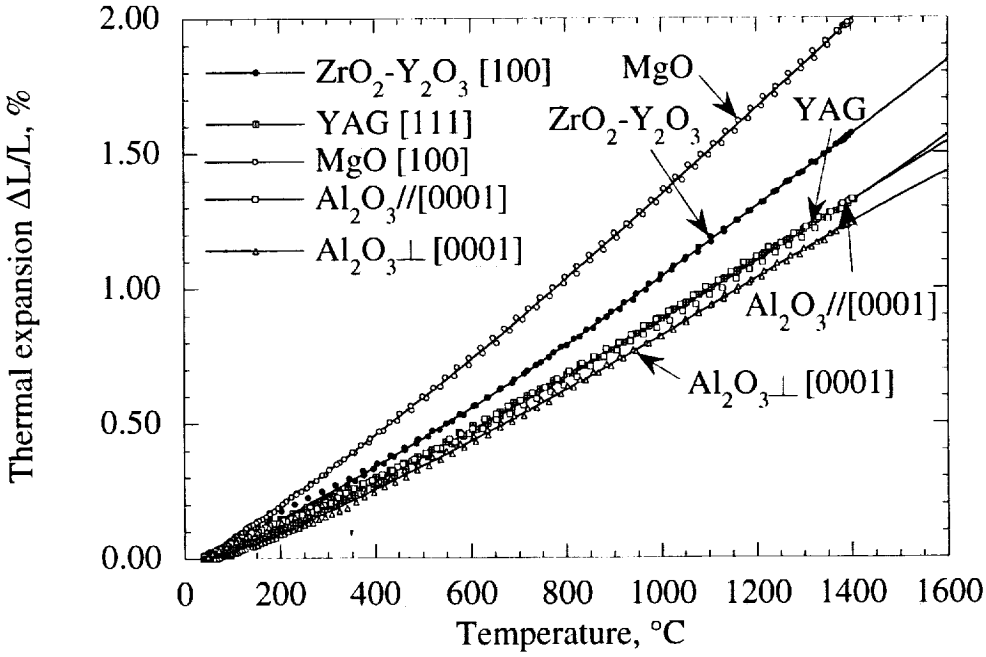

Fig. 3 Thermal expansion behavior of single crystal Y_2O_3-doped ZrO_2, YAG, MgO, and Al_2O_3 (sapphire) oxides.

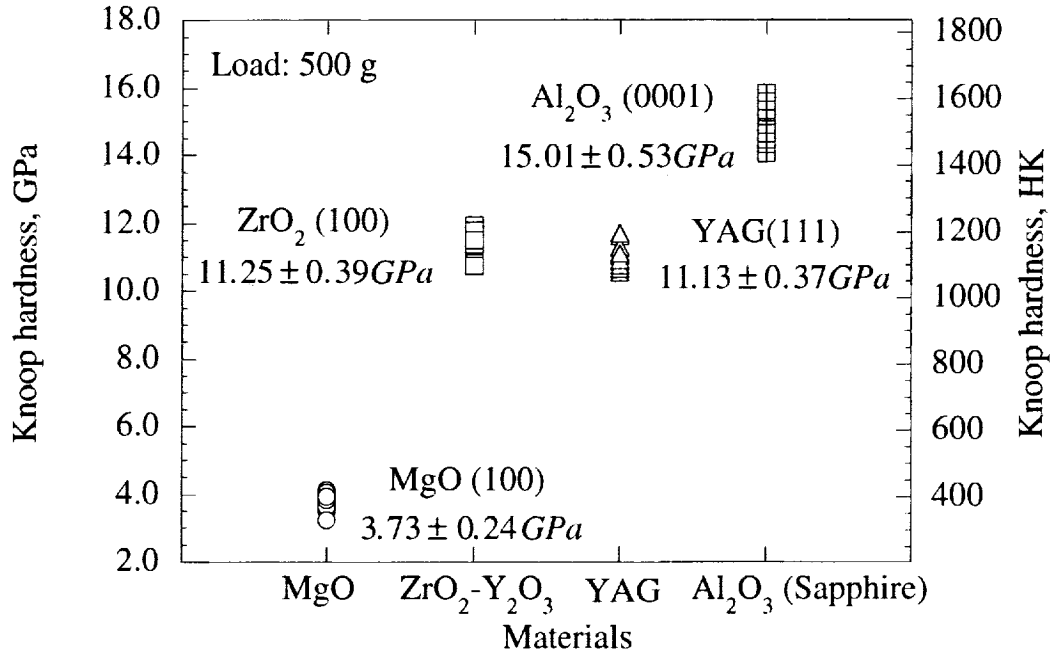

Fig. 4 Knoop hardness measurement results of single crystal Y_2O_3-doped ZrO_2, YAG, MgO, and Al_2O_3 (sapphire) oxides.

Figure 5 illustrates examples of the heating profiles of the Y_2O_3-doped ZrO_2, YAG, and Al_2O_3 (sapphire) disk specimens during the laser steady-state thermal gradient testing. The critical temperature difference and corresponding power density to cause failure were readily determined at the onset of specimen cracking. The test results for all the specimens are shown in Figure 6. The Y_2O_3-doped ZrO_2 and YAG oxides exhibited a similar thermal stress resistance, with the average critical temperature differences being $81 \pm 20°C$ and $88 \pm 21°C$, respectively. In contrast, the Al_2O_3 oxide showed a much better thermal stress resistance. The critical temperature difference for Al_2O_3 was $200 \pm 35°C$. The Al_2O_3 specimens also exhibited a higher thermal stress resistance at higher temperatures. The critical laser power densities at failure for Y_2O_3-doped ZrO_2, YAG and Al_2O_3 disk specimens were approximately 21 W/cm^2, 72 W/cm^2 and 177 W/cm^2, respectively. Note that the critical power density values are corresponding to the total

absorbed laser light energy in the crystals. Considering that thermal gradients established in the secondary solar concentrator systems are due to the heat receiver cavity heating/cooling cycles [3] and to a small portion of solar light energy absorbed in the crystal components, the information obtained from this experiment can be of great importance in component design.

Since the temperature gradient in the specimen resulting from the steady-state heating will impose a compressive stress state in the surface region of the disk specimen, tensile stress would usually be generated near the backside of the specimen. Crack initiation is thus likely to occur near the back surface for the thin specimen, because oxides are much weaker in tension than in compression. The fractographs from the scanning microscope confirmed this type of failure. Figure 7 illustrates the Y_2O_3-ZrO_2 case. Note that the crack origins were typically observed near the back edges of the specimen. The critical temperature difference, ΔT, across the specimen under the steady state heating condition is closely related to the material strength [7, 8]. It is found that the Vickers or Knoop indentation hardness values for oxide systems are closely related to the oxide apparent atomic volumes of oxygen, and thus, to a certain extent, are reflecting the strength of the interatomic bonding [9]. Therefore, the critical ΔT at the low temperature regime (e.g., below 600°C), is believed to be roughly associated with the measured room-temperature Knoop hardness values. Sapphire (Al_2O_3), which has the highest hardness value, showed the best thermal stress resistance. The increased ΔT for Al_2O_3 specimens at higher temperatures may be related to possible microscale stress relaxation due to the inelastic deformation and the reduced modulus value. Surface polish as well as edge-preparation conditions can also dramatically affect these properties. The complicate effects of the test temperature and specimen preparation conditions may explain the relatively large data scatter observed in this study.

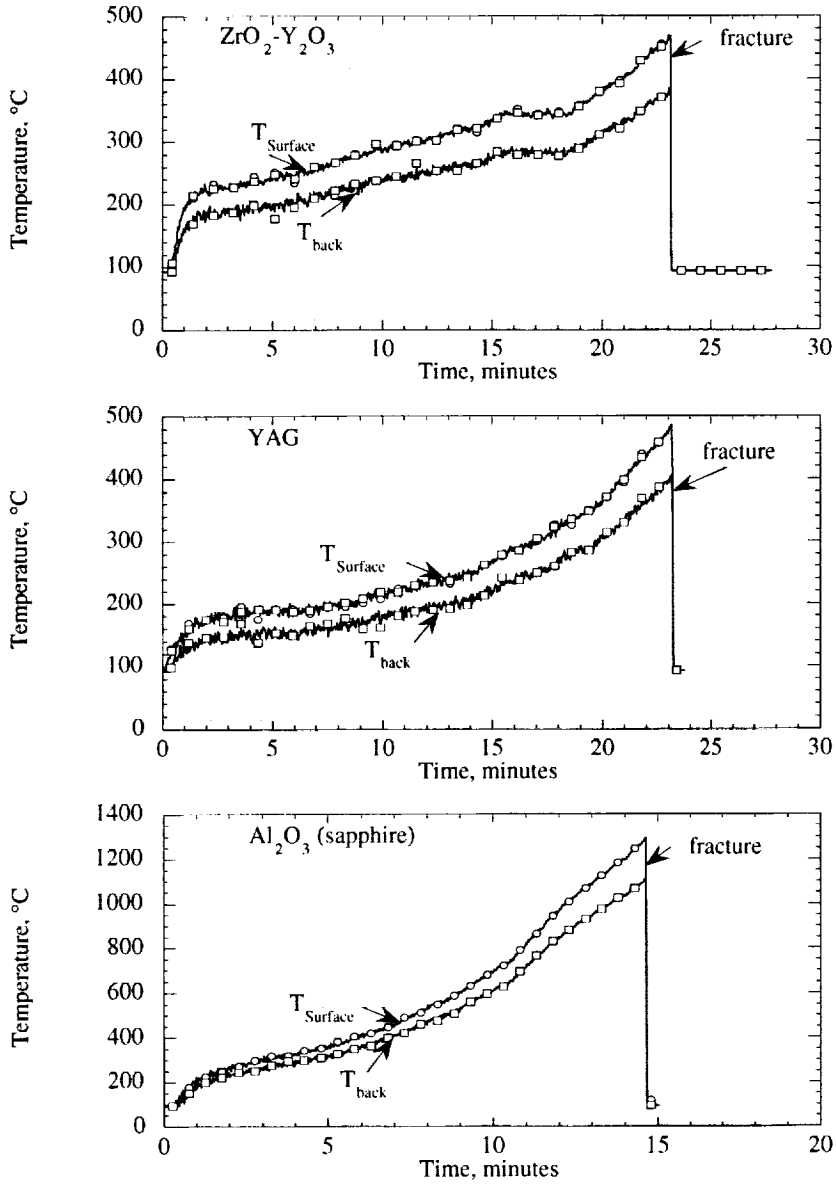

Fig. 5 Examples of the heating profiles of the Y_2O_3-doped ZrO_2, YAG, and Al_2O_3 (sapphire) disk specimens during the laser steady-state thermal gradient testing. The critical temperature difference and corresponding laser power density are thus determined at the onset of cracking.

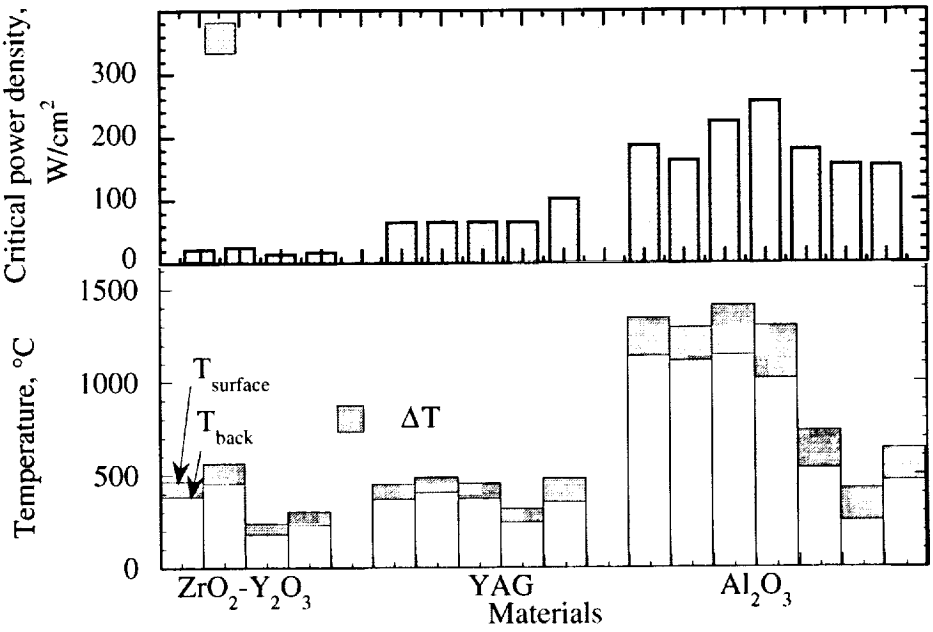

Fig. 6 Critical power densities and critical temperature differences for the Y_2O_3-doped ZrO_2, YAG, and Al_2O_3 (sapphire) disk specimens determined by the laser steady-state thermal gradient testing. The Al_2O_3 showed significantly better thermal stress resistance compared to Y_2O_3-doped ZrO_2 and YAG in terms of the critical temperature difference and power density that cause failure to occur.

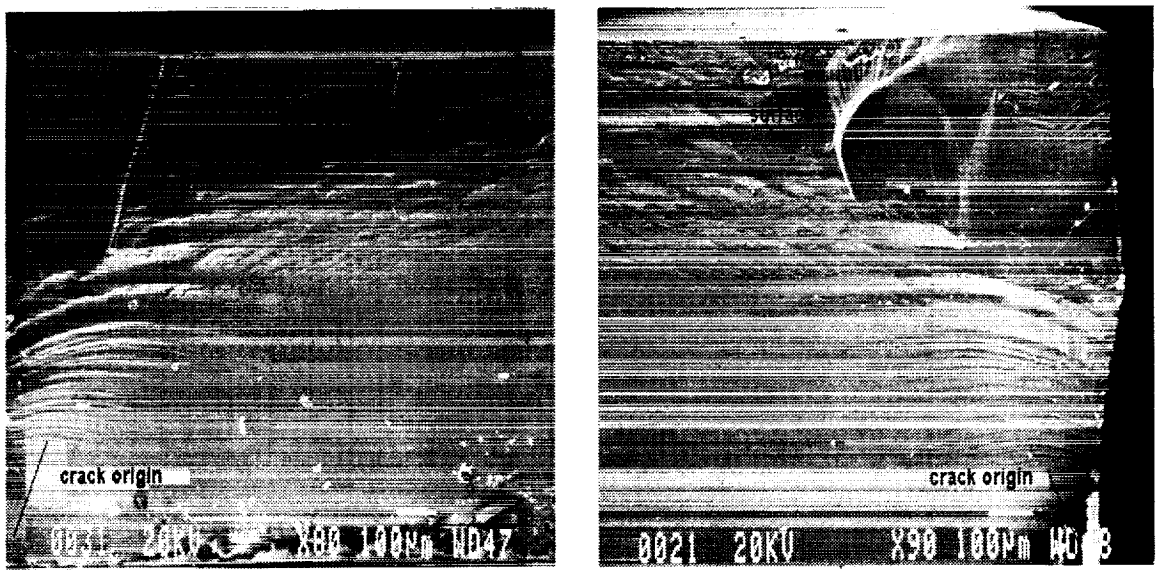

(a) (b)

Fig. 7 SEM fractographs of the Y_2O_3-doped ZrO_2 disk specimens (from two different tests) after the laser steady-state thermal gradient testing. The cracks were initiated near the backside of the specimen surfaces.

Figure 8 shows the temperature profiles of the thermal gradient testing on the single crystal cylindrical specimens under the simulated heating-cooling cycles that may be encountered during the space mission. Maximum temperature differences achieved across the 12.7 mm length were approximately 600°C for Y_2O_3-ZrO_2 and YAG, and 450°C for MgO and Al_2O_3. The temperature gradient was predominantly parallel to the laser heat flux direction, and approximately one-D heating was achieved, as shown in an example of a YAG specimen temperature distribution (Figure 9). The Y_2O_3-ZrO_2 specimen cracked during the second heating cycle. For the MgO specimen, only a small surface crack was initiated after the first test cycle. For both cases, however, the cracks were initiated at the surface during the heating cycle. The YAG and Al_2O_3 specimens did not crack under these test conditions. The cooling cycles seemed to be less damaging for these relatively small size specimens. The Al_2O_3 specimen even survived the quench test (at a cooling rate of 658°C/min) due to the laser power loss in this particular test.

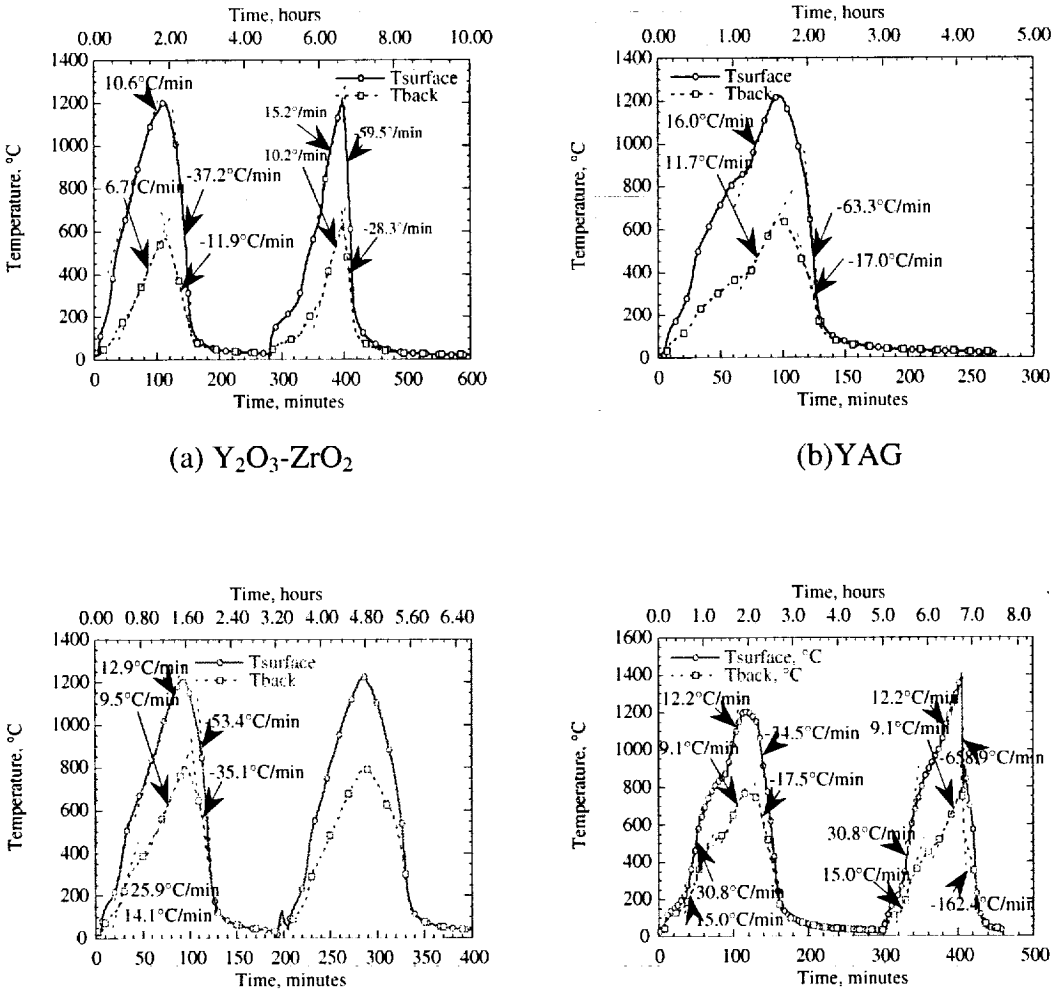

(a) Y_2O_3-ZrO_2 (b)YAG

(c) MgO (d) Al_2O_3

Fig. 8 The thermal gradient testing profiles of the single crystal cylindrical rod specimens to simulate the heating-cooling cycles during the space mission. The maximum heating and cooling rates derived from the temperature-time plots are also labeled in the Figure.

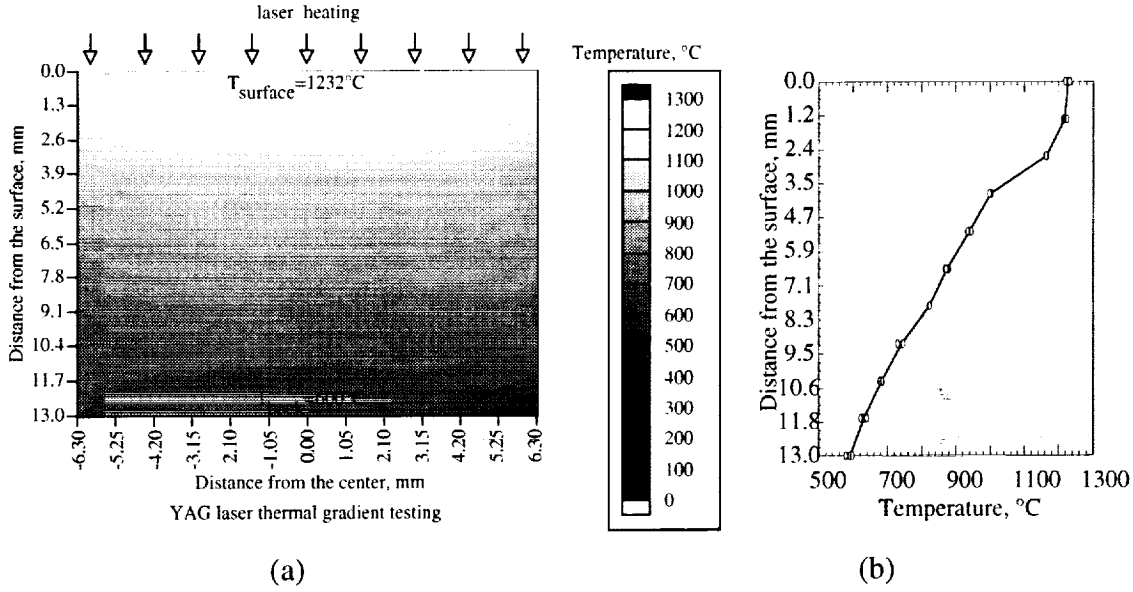

Fig. 9 The thermography temperature distribution in a YAG specimen during the near steady state laser heating (The surface and back side temperatures are approximately 1232°C and 600°C, respectively). (a) Temperature contour distribution in the specimen; (b) temperature distribution along the specimen center region.

For a given material and heating time, the thermal stresses in the specimen increase with the laser power density. Therefore, the critical laser power densities for crystal failure can be determined by laser thermal shock tests under well-controlled transient heating conditions. The results of the laser thermal shock tests showed that the critical power densities at failure were approximately 15.3 W/cm^2, 56.9 W/cm^2, 39.1 W/cm^2 and 109.4 W/cm^2 for Y_2O_3-ZrO_2, YAG, MgO and Al_2O_3 (sapphire) cylindrical specimens, respectively. The Al_2O_3 showed the best thermal shock resistance of all the oxide materials tested. The good thermal shock resistance of sapphire is attributed to its high strength, high thermal conductivity and low thermal expansion coefficient.

The failure modes of the single crystal oxides under laser transient thermal shock conditions are relatively complex. From the experiments, it was observed that, for the materials with low thermal conductivity and high thermal expansion, such as Y_2O_3-ZrO_2

and MgO, the surface cracks could be readily initiated by high compressive stresses and/or the compressive stress-induced (resolved) shear stresses. On the other hand, for the materials with high thermal conductivity and low thermal expansion, such as Al_2O_3 and YAG, the cracks are more likely initiated deep in the crystals. Figure 10 illustrates the thermography temperature distributions of YAG and Al_2O_3 during the laser heating, and the crystal cracking observed in the middle of the cylindrical specimens. Note that a large crack developed in the Al_2O_3 specimen, causing a strong reflection in the thermography image. Therefore, the thermography temperature reading near the crack is no longer valid. Figure 11 illustrates the crack and fracture morphologies of the single crystal oxides after the laser transient thermal shock testing.

For the purpose of demonstration, the stresses in the 12.7 mm long cylindrical specimens have been estimated at the critical laser power densities, based on the temperature distributions measured by thermography and a one-D heat transfer model and under the assumed biaxial stress condition. The material properties used in calculations are listed in Table 1. The results are illustrated in Figure 12. Note that for the much thicker specimen under the transient heating conditions, the stress distributions in the specimen are different from those in the thin specimen case described earlier. In the thick specimen case, after heating up the crystal, a high compressive stress is developed near the surface. The surface compressive stress decreases with the heating time. However, the tensile stress in the inner layer of the crystal increases with time (Figure 12). The peak tensile stress quickly reaches the maximum value and remains almost constant, but it shifts towards the surface for longer time. The backside of the specimen is in compression. It is believed that the surface compressive stress and near-surface tensile stresses are responsible for the observed crystal failures under the laser transient heating conditions.

Table 1. The material properties (average values in the temperature range of 25°C to 1000°C) [7, 10-12] used in thermal stress calculations

Materials	Density, g/cm^3	Heat capacity C_p, J/g-K	Thermal conductivity, W/cm-K	Thermal expansion coefficient α, m/m-K	Young's modulus, E GPa	Poission's ratio, ν
ZrO_2-Y_2O_3	5.236	0.582	0.02	10.6×10^{-6}	210	0.25
YAG	4.554	0.612	0.082	9.2×10^{-6}	277.5	0.25
MgO	3.585	1.005	0.052	13.7×10^{-6}	245	0.3
Al_2O_3	3.38	1.15	0.12	8.6×10^{-6}	380	0.22

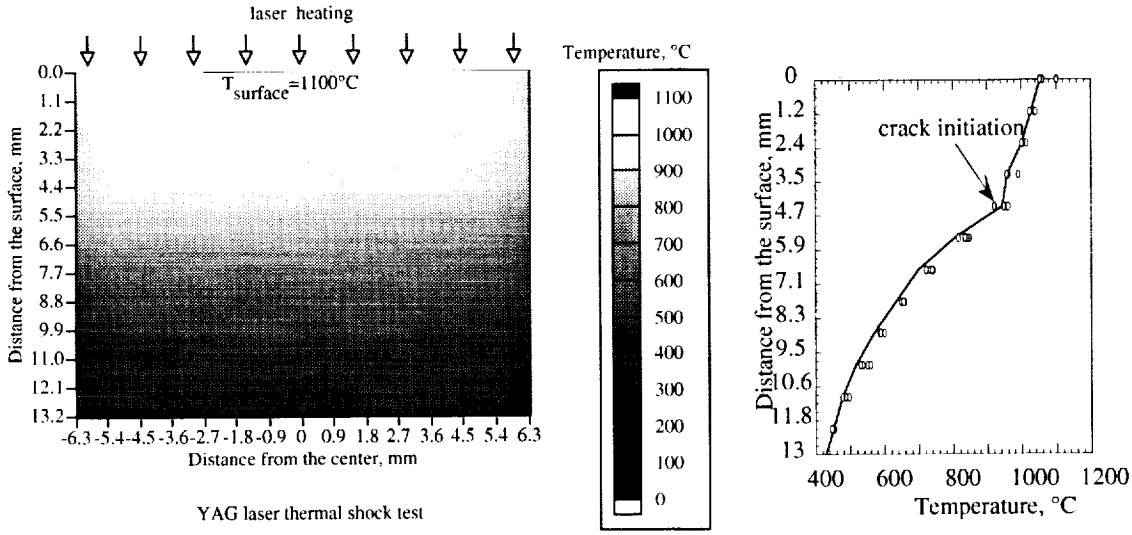

(a) (b)

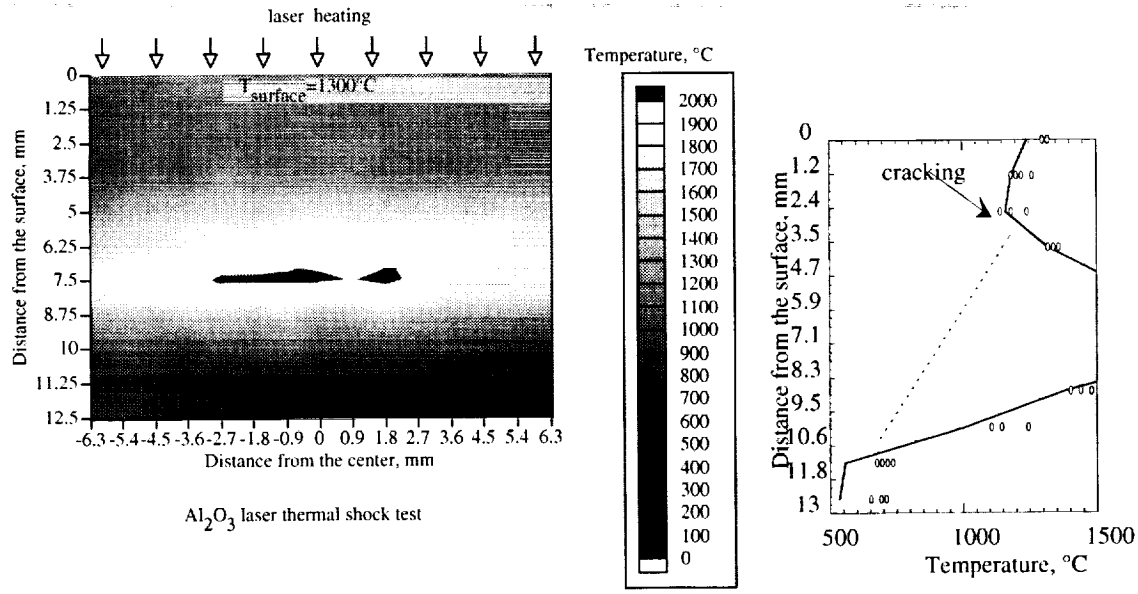

(c) (d)

Fig. 10 The temperature distributions in YAG and Al_2O_3 specimens during the laser thermal shock testing after 50 sec heating at the critical laser powers. (a and b) Temperature contour and line distributions in YAG; (c and d) temperature contour and line distributions in Al_2O_3.

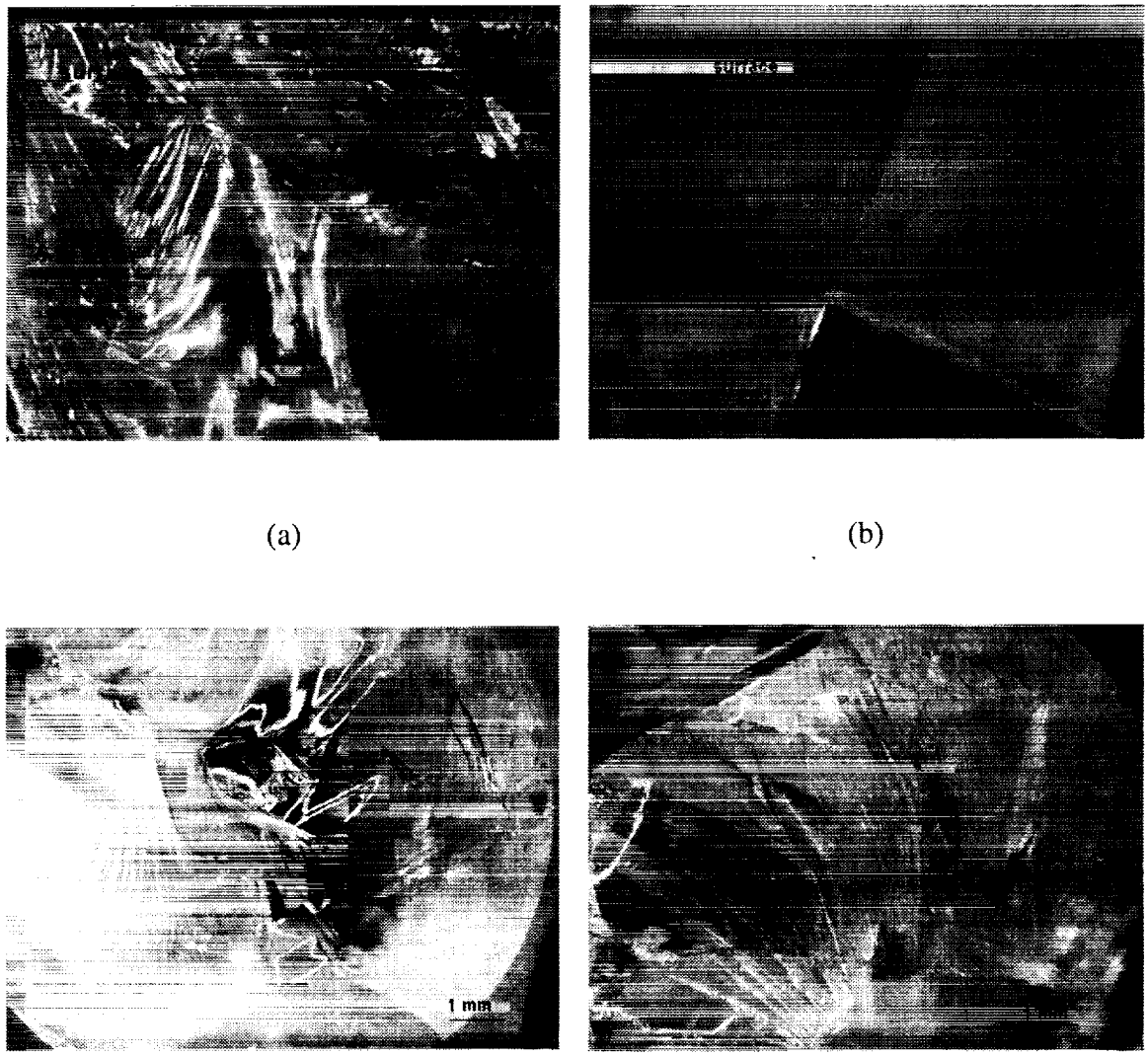

Fig. 11 The crack and fracture morphologies (optical microscopy) of the single crystal oxides after the laser thermal transient testing. (a) Surface initiated cracks and the subsequent crack propagation in ZrO_2-Y_2O_3; (b) surface shear stress initiated cleavage along the (110) plane in MgO; (c) the cracked surface in the middle of the YAG specimen; (d) the cracked surface in the middle of the Al_2O_3 specimen.

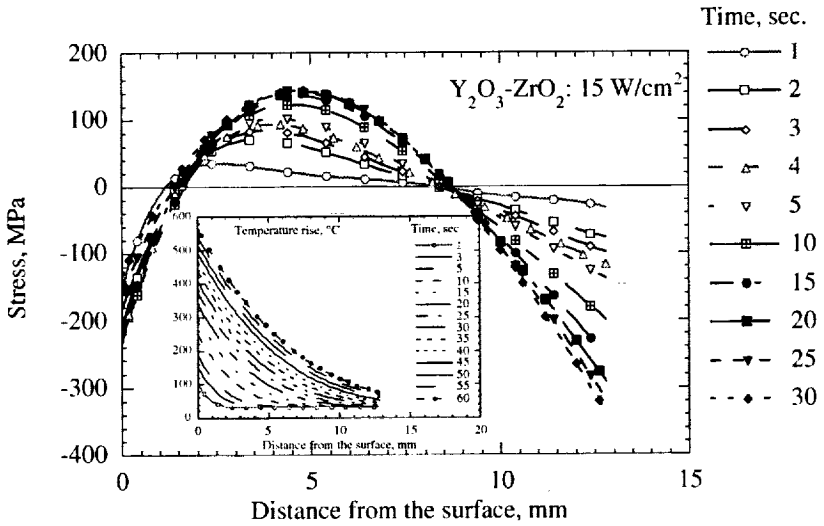

(a) Y_2O_3-ZrO_2

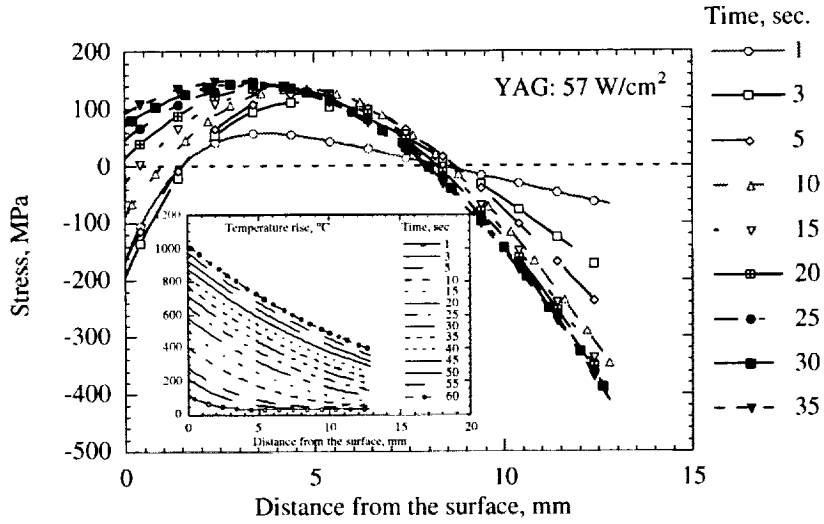

(b) YAG

Fig. 12 The modeled thermal stress distributions in the 12.7 mm long cylindrical specimens during laser transient thermal shock testing at the critical laser power densities.

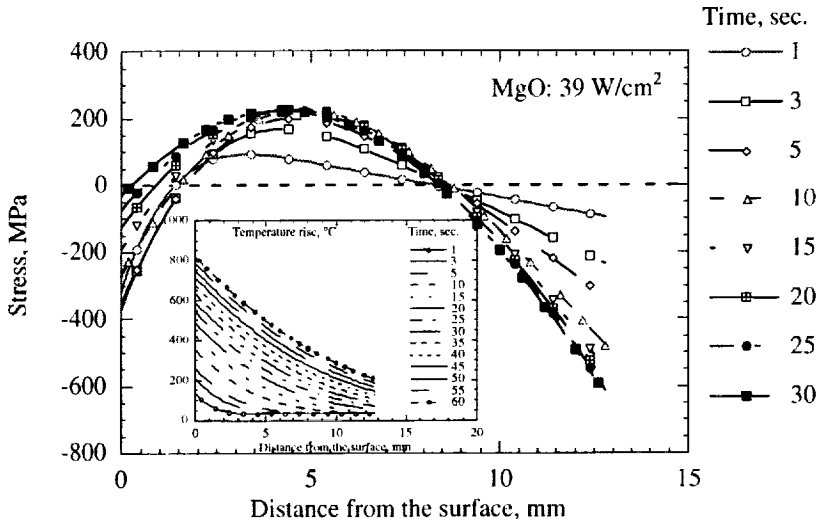

(c) MgO

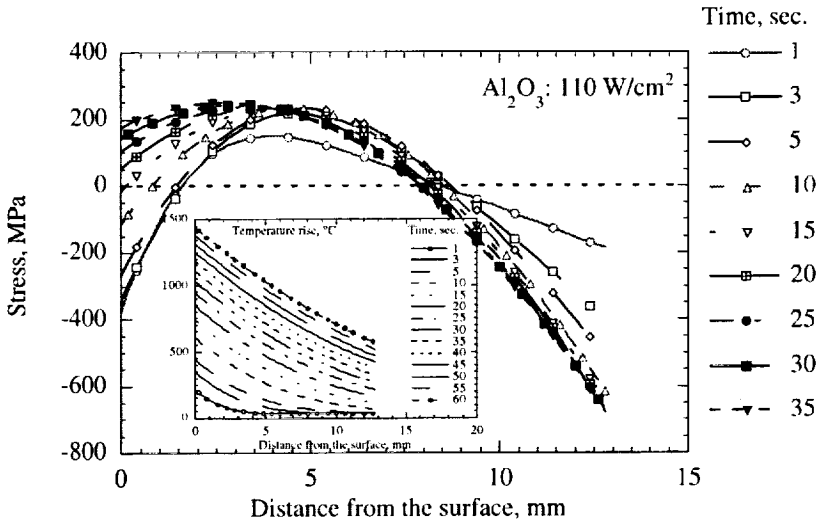

(d) Al_2O_3

Fig. 12 (Continued) The modeled thermal stress distributions in the 12.7 mm long cylindrical specimens during laser transient thermal shock testing at the critical laser power densities.

CONCLUDING REMARKS

A laser thermal shock test approach has been proposed for evaluating thermo-mechanical stability of single crystal oxide refractive concentrator materials under simulated mission conditions. This technique is especially useful in determining the thermal stress resistance of single crystal oxides under steady state and transient thermal heating, thus providing vital information for the component design and material development.

Thermal shock resistance of several candidate single crystal oxide concentrator materials, namely yttria-stabilized zirconia, yttrium aluminum garnet and magnesium oxide and sapphire was investigated. The experiments showed that the single crystal sapphire can sustain the highest temperature gradient and heating-cooling rate, as compared to the other oxides, thus exhibiting the best thermal shock resistance.

ACKNOWLEDGMENTS

This work was supported by NASA Lewis Research Center Refractive Secondary Solar Concentrator development project, and NASA Marshall Space Flight Center shooting Star Program. The authors are grateful to Robert P. Macosko for valuable discussions.

REFERENCES

[1] J. A. Soules, D. R. Buchele, C. H. Castle, and R. P. Macosko, "Design and Fabrication of a Dielectric Total Internal Reflecting Solar Concentrator and Associated Flux Extractor for Extreme High Temperature (2500K) Applications," NASA Lewis Research Center, Cleveland, NASA CR 204145, November 1997.

[2] X. Ning, R. Winston, and J. O'Gallagher, "Dielectric Totally Internally Reflecting Concentrators," *Applied Optics*, vol. 26, pp. 300-305, 1987.

[3] S. M. Geng, "Transient Thermal Heat-up of a Refractive Secondary Solar Concentrator," *To be published*, 1998.

[4] J. T. Luxon and D. E. Parker, *Industrial Lasers and Their Applications*. Englewood Cliffs, New Jersey: Prentice-Hall, Inc., 1985.

[5] D. Zhu and R. A. Miller, "Thermal Fatigue Testing of ZrO_2-Y_2O_3 Thermal Barrier Coating Systems using A High Power Laser," NASA Lewis Research Center, Cleveland, Technical Memorandum 107439, June 1997.

[6] D. Zhu and R. A. Miller, "Investigation of Thermal High Cycle and Low Cycle Fatigue Mechanisms of Thick Thermal Barrier Coatings," *Materials Science and Engineering*, vol. A245, pp. 212-223, 1998.

[7] W. D. Kingery, "Factors Affecting Thermal Stress Resistance of Ceramic Materials," *Journal of the American Ceramic Society*, vol. 38, pp. 3-15, 1955.

[8] D. P. Hasselman, "Thermal Stress Resistance of Engineering Ceramics," *Materials Science and Engineering*, vol. 71, pp. 251-264, 1985.

[9] W. B. Hillig, "A Methodology for Estimating the Mechanical Properties of Oxides at High Temperature," *Journal of the American Ceramic Society*, vol. 76, pp. 129-138, 1993.

[10] "Nd^{3+}: $Y_3Al_5O_{12}$ (YAG) Physical Properties," *personal communication*, 1997.

[11] W. P. Holbrook, J. B. Wachtman, C. Schnitzer, and L. M. Sheppard, "Ceramic Source," vol. 8, 1992-1993.

[12] D. Zhu and R. A. Miller, "Investigation of Thermal Fatigue Behavior of Thermal Barrier Coating Systems," *Surface and Coatings Technology*, vol. 94-95, pp. 94-101, 1997.

REPORT DOCUMENTATION PAGE

Form Approved
OMB No. 0704-0188

1. AGENCY USE ONLY (*Leave blank*)	2. REPORT DATE	3. REPORT TYPE AND DATES COVERED
	February 1999	Technical Memorandum

4. TITLE AND SUBTITLE

Thermal-Mechanical Stability of Single Crystal Oxide Refractive Concentrators for High-Temperature Solar Thermal Propulsion

5. FUNDING NUMBERS

WU-953-73-10-00

6. AUTHOR(S)

Dongming Zhu, Nathan S. Jacobson, and Robert A. Miller

7. PERFORMING ORGANIZATION NAME(S) AND ADDRESS(ES)

National Aeronautics and Space Administration
Lewis Research Center
Cleveland, Ohio 44135-3191

8. PERFORMING ORGANIZATION REPORT NUMBER

E-11524

9. SPONSORING/MONITORING AGENCY NAME(S) AND ADDRESS(ES)

National Aeronautics and Space Administration
Washington, DC 20546-0001

10. SPONSORING/MONITORING AGENCY REPORT NUMBER

NASA TM—1999-208899

11. SUPPLEMENTARY NOTES

Prepared for the 1999 International Solar Energy Conference, Renewable and Advanced Energy Systems for the 21st Century sponsored by the American Society of Mechanical Engineers, Lahaina, Maui, Hawaii, April 11-15, 1999. Responsible person, Dongming Zhu, organization code 5160, (216) 433-5422.

12a. DISTRIBUTION/AVAILABILITY STATEMENT

Unclassified - Unlimited
Subject Categories: 23 and 20 Distribution: Nonstandard

This publication is available from the NASA Center for AeroSpace Information, (301) 621-0390.

12b. DISTRIBUTION CODE

13. ABSTRACT ***(Maximum 200 words)***

Single crystal oxides such as yttria-stabilized zirconia (Y_2O_3-ZrO_2), yttrium aluminum garnet ($Y_3Al_5O_{12}$, or YAG), magnesium oxide (MgO) and sapphire (Al_2O_3) are candidate refractive secondary concentrator materials for high temperature solar propulsion applications. However, thermo-mechanical reliability of these components in severe thermal environments during the space mission sun/shade transition is of great concern. Simulated mission tests are important for evaluating these candidate oxide materials under a variety of transient and steady-state heat flux conditions, and thus provide vital information for the component design. In this paper, a controlled heat flux thermal shock test approach is established for the single crystal oxide materials using a 3.0 kW continuous wave CO_2 laser, with a wavelength 10.6 micron. Thermal fracture behavior and failure mechanisms of these oxide materials are investigated and critical temperature gradients are determined under various temperature and heating conditions. The test results show that single crystal sapphire is able to sustain the highest temperature gradient and heating-cooling rate, and thus exhibit the best thermal shock resistance, as compared to the yttria-stabilized zirconia, yttrium aluminum garnet and magnesium oxide.

14. SUBJECT TERMS	15. NUMBER OF PAGES
Single crystal oxides; Solar concentrators; High temperature thermal gradient testing	28
	16. PRICE CODE A03

17. SECURITY CLASSIFICATION OF REPORT	18. SECURITY CLASSIFICATION OF THIS PAGE	19. SECURITY CLASSIFICATION OF ABSTRACT	20. LIMITATION OF ABSTRACT
Unclassified	Unclassified	Unclassified	